Super Dual Auroral Radar Network observations of velocity-divergent structures in the F region ionosphere

R. André, Jean- Pierre Villain, V. Krassnosel'Skikh, C. Hanuise

JOURNAL OF GEOPHYSICAL RESEARCH, VOL. 105, NO. A9, PAGES 20,899–20,908, SEPTEMBER 1, 2000

Super Dual Auroral Radar Network observations of velocity-divergent structures in the *F* region ionosphere

R. André, J.-P. Villain, and V. Krassnosel'skikh

Laboratoire de Physique et Chimie de l'Environnement, Centre National de la Recherche Scientifique Orléans, France

C. Hanuise

Laboratoire de Sondage de l'Environnement Electromagnétique Terrestre, Centre National de la Recherche Scientifique, Université de Toulon et du Var, La Garde, France

Abstract. This paper describes Super Dual Auroral Radar Network observations of an unusual mesoscale (scale size $L \approx 300$ km) structure in the auroral convection pattern. This structure is characterized by an expansion motion of the plasma in a plane perpendicular to the magnetic field and then by an anomalously high velocity divergence. This study describes those observations and eliminates possible artifacts in the data analysis. Because the radar data strongly suggest that the structure is located in the *F* region, the observations are thus in opposition with the well-known divergence-free motion hypothesis. They are interpreted in terms of an ion demagnetization process, in which the collisionless ions become locally collisional in the *F* region.

1. Introduction

The Super Dual Auroral Radar Network (SuperDARN) network of HF radars [*Greenwald et al.*, 1995b] is mainly devoted to ionospheric convection studies and gives a large-scale view of the solar-terrestrial interactions. Previous studies have shown global convection patterns during various solar wind conditions [e.g., *Greenwald et al.*, 1995a; *Ruohoniemi and Greenwald*, 1996]. If the interplanetary magnetic field (IMF) conditions produce the main forcing on the ionospheric convection pattern, several perturbations can affect it and could add smaller-scale structures to the basic pattern. For example, flux transfer events (FTE) [*Russell and Elphic*, 1978] and travelling convection vortices (TCV) [*Friis-Christensen et al.*, 1988] produce a moving field-aligned current system and then superimpose a double-vortex signature on the ionospheric convection. Such events are the source of perturbations in the ionospheric convection pattern, at several scale sizes, from large ones as for the substorms to medium ones for FTE or TCV to smaller ones. The characterization of those events is of great importance to our knowledge of solar-terrestrial relations.

Computing velocity vectors with the standard method [*Cerisier and Senior*, 1994], the SuperDARN instrument is able to resolve structures in the convection which have a scale size (L) of the order of 500 km. Some recent developments [*André et al.*, 1999] have optimized this method in order to produce high-resolution convection maps and give access to smaller structures ($L \approx 200$ km).

Paper number 1999JA900492.
0148-0227/00/1999JA900492$09.00

Applying this technique to various data sets, we found several unusual mesoscale structures ($L \approx 300$ km) characterized by an anomalous divergence in the velocity field. This property is unexpected in the *F* region, where the structure is supposed to be observed and a divergence-free motion is expected [*Ruohoniemi et al.*, 1989]. Section 2 discusses extensively the geophysical context of one event and summarizes the other observations. Then SuperDARN data are carefully analyzed, and a possible anomalous radar wave propagation is considered in order to reject the possibility of any artifact.

Section 3 formulates the physical problem introduced by those observations and shows that a local ion demagnetization in which the effective ion collision frequency is greater than the gyrofrequency is the most appropriate answer. In this process, the collisionless *F* region ions become collisional, and their motion becomes highly divergent under the observed divergent electric field. Finally, we discuss the large increase in collision frequency and suggest that a crucial role is played by an anomalous ion transport.

2. SuperDARN Observations

Six events characterized by a highly divergent structure have been found in the SuperDARN data set for 1995. In this section one of them is extensively described, with a particular emphasis on the global geophysical context. Then the other observations are summarized, and finally, the possibility of a measurement artifact is discussed and discarded.

2.1. Extensive Description of One Event

The event presented here has been recorded on February 17, 1995, around 2230 UT. Since the main convection forc-

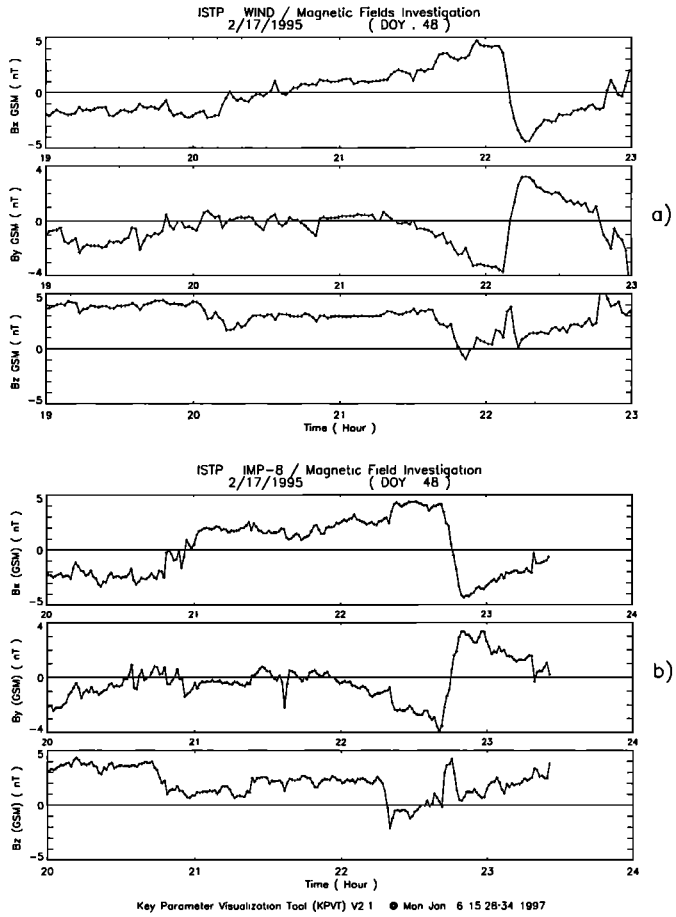

Figure 1. Interplanetary magnetic field recorded on board (a) WIND and (b) IMP 8.

ing is originating from the solar wind, we first examined the IMF data recorded by the satellites WIND and IMP 8.

2.1.1. Solar wind conditions. During the period of interest (1900-2000 UT) the WIND satellite was located in the solar wind at $x \approx +200\ R_E$, $y \approx -30\ R_E$ and $z \approx -13\ R_E$ in GSM coordinates. Figure 1a shows the IMF recorded between 1900 and 2300 UT. The B_z component is northward and has a moderate amplitude (+3-4 nT) for several hours. At 2150 UT it turns slowly southward and turns back northward 10 min later. The B_y component is negative for 1 hour with a small amplitude (2 nT) between 1900 and 2000 UT. Then, it slowly varies around 0 nT and progressively decreases at $\sim$ 2130 UT. The B_x component is first negative for 90 min with an amplitude of -2 nT and increases regularly to +4 nT when B_z is negative. The solar wind velocity during this period is constant and of the order of 400 km/s. The main change in the solar wind conditions is then the southward turning of the IMF.

The IMP 8 satellite is also located in the solar wind at $x \approx +34\ R_E$, $y \approx +2.5\ R_E$, and $z \approx +14\ R_E$, in front of the magnetosphere. Figure 1b shows the magnetic field recorded onboard. Its characteristics are similar to the WIND data but are observed with a time delay of the order of 25 min.

Three different periods can be distinguished. The first one, between 2100 and 2200 UT (for the IMP 8 satellite), is characterized by a steady magnetic field with $B_x \approx +2$ nT, $B_y \approx 0$ nT, and $B_z \approx +2$ nT. The B_y component does not favor reconnection on one side of the magnetosphere [*Reiff and Burch*, 1985], and the B_x suggests a lobe reconnection on the South Pole only [*Crooker*, 1992; *Crooker and Rich*, 1993]. During this period the ionospheric convection pattern should have four cells in the Southern Hemisphere and two cells in the Northern Hemisphere which are induced by the viscous interaction with the solar wind. In this hemisphere we expect an irregular convection pattern in the nightside ionosphere.

The second period is defined between 2200 and 2220 UT with the IMP 8 timescale. The IMF components are $B_x \approx +3$ nT and $B_z \approx +2$ nT. Those components are in favor of a two-cells convection pattern in the Northern Hemisphere. The B_y component decreases slowly toward a negative value of -2 nT, which suggests a reconnection on the dawnside of the magnetosphere. The expected convection pattern should then change from a two-cells to a three-cells scheme.

Finally, the third period is defined between 2220 and 2235 UT, when the IMF has the components $B_x \approx +4$ nT, $B_y \approx -2$ nT, and $B_z \approx -1$ nT. Here the magnetic field reconnection rate should increase because of the southward turning, and the convection pattern should have two cells. The dawn cell should be more important owing to the negative B_y component.

The most important change is the southward turning of the IMF, and the convection pattern should reflect this global evolution with a time delay. Following the analysis of *Lester*

et al. [1993], *Ruohoniemi et al.* [1993], and *Taylor et al.* [1994], we shall evaluate this delay. The convection pattern should have two cells between 2125 and 2225 UT, and then we expect the appearance of a third one in the dawn sector between 2225 and 2245 UT. Finally, between 2245 and 2310 UT the convection should be controlled by the southward IMF and then have two larger cells.

2.1.2. Large-scale convection observed with SuperDARN. Using the SuperDARN data from the Saskatoon/Kapuskasing radar pair and the Goose Bay/Stokkseyri radar pair, we have mapped the velocity vectors with the standard computational method [*Cerisier and Senior*, 1994] for > 7 hours of magnetic local time (MLT).

The map presented in Figure 2 shows the time-averaged convection map (over ~ 10 min) defined in geomagnetic coordinates at ~ 2210 UT and thus corresponds to the first period. The dayside convection is characterized by a vortex located near 78°magnetic latitude (MLAT), with a longitudinal extension of ~ 3 hours (between 14 and 17 MLT). This vortex indicates the presence of an upward field-aligned current and should be related to viscous interaction between the solar wind and the magnetosphere. Despite its high-latitude location this vortex could be located on closed magnetospheric field lines. In the duskside sector, between the invariant magnetic latitudes 77°and 82°, the sunward convection cannot be associated with the current system generated by lobe reconnection [*Kamide and Troshichev*, 1994]. This convection pattern should be located on closed magnetic field lines too. At 2000 MLT and 73°, there is a velocity shear, and at ~ 2100 MLT and 75°, there is a convection reversal. Those structures are in good agreement with the irregular convection pattern observed in the nightside ionosphere during periods of northward IMF [*Bythrow et al.*, 1985; *Cumnock et al.*, 1995]. Despite the fact that the convection is not observed on the full hemisphere, one concludes that this pattern is in good agreement with the previous IMF observations.

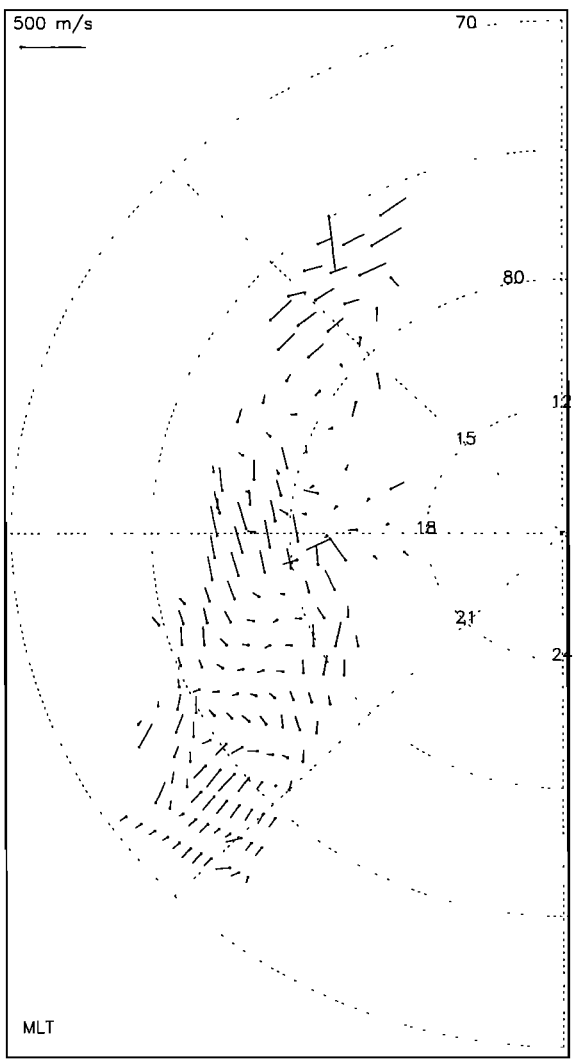

Figure 2. Velocity vector map determined by SuperDARN in the Northern Hemisphere at ~ 2210 UT, February 17, 1995.

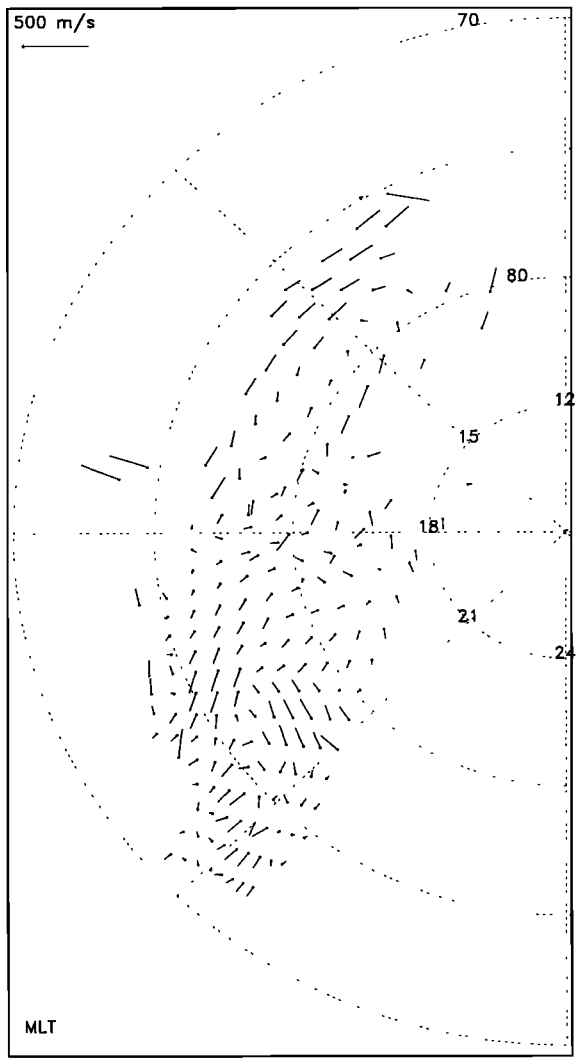

Figure 3. Velocity vector map determined by SuperDARN in the Northern Hemisphere at ~ 2230 UT, February 17, 1995.

Figure 3 shows the convection recorded by the same radar pairs nearly 20 min later, around 2230 UT. This convection corresponds to the second IMF period. First, the dayside

vortex is nearly identical. In the dusk sector the convection pattern has changed. The plasma is now flowing equatorward and, at ~ 1930 MLT and above 80°, is moving in the antisunward direction. This modification is attributed to a global change in the solar wind/magnetosphere coupling. During this period the B_y component is decreasing to -1 nT. Following *Tagushi and Hoffman* [1996], an IMF clock angle ($\arctan(|B_y|/B_z)$) > 30°suggests a reconnection on the flank of the magnetosphere. In our case, the clock angle is going from 15°at ~ 2210 UT to 60°at 2230 UT. We can therefore suppose that the new orientation modifies the convection pattern. Moreover, the negative B_y suggests the presence of an counter-clockwise cell in the dawn sector [*Heelis et al.*, 1986], which is in agreement with the antisunward convection pattern observed at high latitudes. The observations are again in good agreement with the expectations for this period.

Finally, at ~ 2100 MLT and 75°MLAT the velocity shear seems to disappear in order to form a small structure characterized by a large velocity divergence. These observations suggest that this structure appears just after a global change in the solar wind magnetosphere coupling.

2.1.3. Velocity-divergent structure. The high-resolution merging method [*André et al.*, 1999] gives more details on the velocity-divergent structure. Figure 4 shows a part of the convection pattern, as seen by the Goose Bay/Stokkseyri radar pair. These maps are averaged in time for two scans (192 s). The structure is located at 75°MLAT and 2100 MLT and is characterized by a velocity divergence of the order of 7 mHz. This is ~ 1 order of magnitude greater than the typical values (< 1 mHz), which are introduced by measurement uncertainties. Its typical scale size is of the order of 200 km, and its distance from the radars is 1200 and 2000 km, respectively. This means that this structure should be located in the *F* region, where the plasma motion is supposed to be divergence-free.

2.1.4. Temporal evolution. In order to characterize the structure formation we have computed the temporal evolution of the convection with the standard resolution. The result is presented in Figures 5a to 5f. Each plot shows the mean convection pattern for a period of ~ 6 min (four radar scans).

At ~ 2205 UT (Figure 5a) the convection pattern is mostly in the sunward direction. Plasma velocities are regular with an amplitude of ~ 100 m/s for the lowest magnetic latitudes and become untidy at higher latitudes, with smaller amplitudes (< 100 m/s). Ten minutes later (Figure 5b), the plasma motion in the 2100 MLT and 74°MLAT sector is now clearly antisunward. Everywhere else, the plasma is still moving sunward and seems to be driven by a higher electric field. Between these two regions, one can define a small boundary in which the plasma velocity is equatorward. Figure 5b strongly suggests the presence of an electric field shear. At 2215 and 2220 UT (Figures 5c and 5d) this boundary is moving sunward, and a convection reversal appears in the sector 2100 MLT, 76°MLAT. These observations are indicative of the formation of a downward field-aligned current, related to the tailward motion of an electric field shear in the magnetosphere.

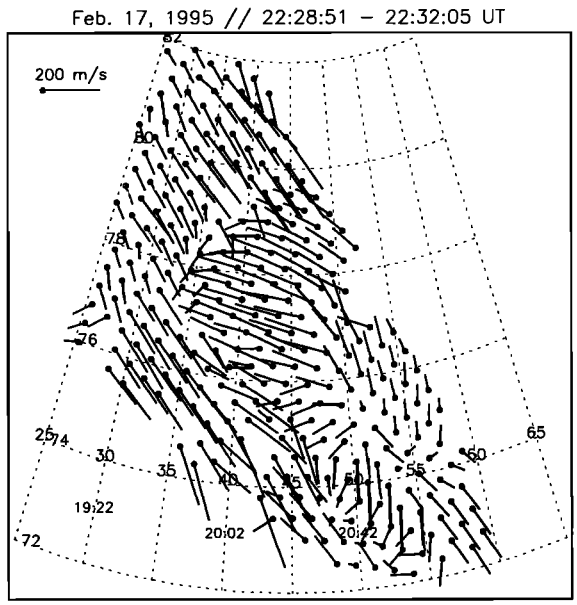

Figure 4. Velocity-divergent structure defined by the Goose Bay/Stokkseyri pair.

At 2228 UT (Figure 5e) the sunward convection has totally disappeared from the radar field of views. The convection reversal has become a velocity-divergent structure which seems to be superimposed on an antisunward convection pattern. The structure seems to remain steady for ~ 10 min (Figure 5f), and one notes the growth (size and amplitude) of the electric field located in the sector 2000 MLT and 77°MLAT. At higher latitudes the convection is now sunward again.

This temporal evolution corresponds to the development of an electric field shear in the magnetosphere, which is moving toward the magnetotail. Then, the formation of a convection reversal in the velocity field indicates the presence of a divergent electric field structure and an associated downward field-aligned current. A few minutes later, the plasma motion becomes highly divergent in its center, this unusual structure being observed for 10 min.

2.1.5. Signal-to-noise ratio recorded by the Stokkseyri radar. Another method is to check the associated signal-to-noise ratio (SNR). This quantity is proportional to the electron density and to the amplitude of the 15-m-scale electron density irregularities. Several mechanisms enhance or reduce this quantity, such as turbulence level, electron precipitations, or radar wave absorption. Figures 6a to 6f show the SNR evolution recorded by the Stokkseyri radar during the event. These maps are plotted in geomagnetic coordinates with a temporal resolution of 96 s. The selected scans are comparable to Figures 5a to 5f.

At 2205 UT (Figure 6a) a high SNR area (SNR > 25 dB) located at ~ 2100 MLT and 75°MLAT is present. This area expands with time (Figures 6b and 6c) and splits into two parts at ~ 2220 UT (Figure 6d). One of them moves to higher latitudes (Figure 6e), and at 2235 UT the size of both increase (Figure 6f).

The two areas are located exactly on the boundary of the convection reversal (Figures 6c and 6d) and of the high-

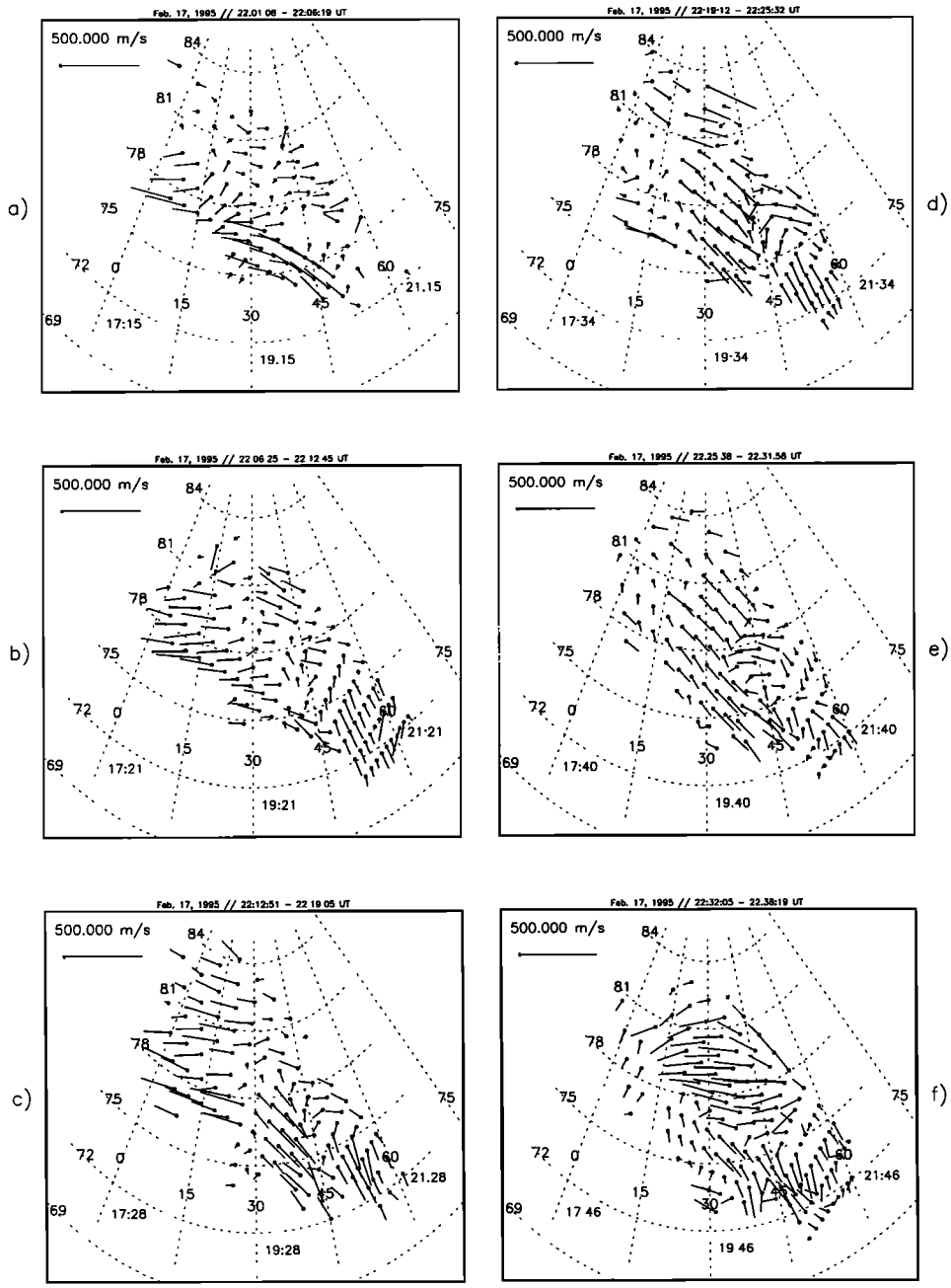

Figure 5. Temporal evolution of the convection determined by the Goose Bay / Stokkseyri radars

velocity divergence structure (Figures 6e and 6f). Moreover, their evolutions are well correlated with their dynamics. It is quite probable that irregularities with scale size of 15 m are greatly enhanced at the boundary of a larger structure, i.e., convection reversal or high-velocity divergence structure, which contains density gradients [*Tsunoda*, 1988]. So their evolutions are related to the dynamic of the field-aligned current and its associated divergent electric field structure. The scale size of the structure is of the order of 700 km in the radar beam direction.

2.1.6. Ground magnetic activity. During the event the planetary magnetic activity is very quiet ($Kp = 1^+$). Since the IMF is northward and the magnetic activity is very low, the size of the auroral oval is very small [*Siscoe*, 1991]. This agrees with previous large-scale convection observations.

The magnetometers located on the Greenland west coast are in the field of view of the Goose Bay/Stokkseyri radar pair but are located 250 km away from the high-velocity divergence structure. They do not show any magnetic perturbation (maximum < 20 nT) and so do not record any large-scale field-aligned current. This emphasizes the small-scale size of the structure.

2.2. Observations Summary

The 1995 SuperDARN data have been examined, and similar structures have been found five times. Their characteristics are summarized in Table 1. The IMF is northward for all of them. The clock angle has no particular value, and the convection pattern is different from one event to another. The planetary magnetic activity is always very small

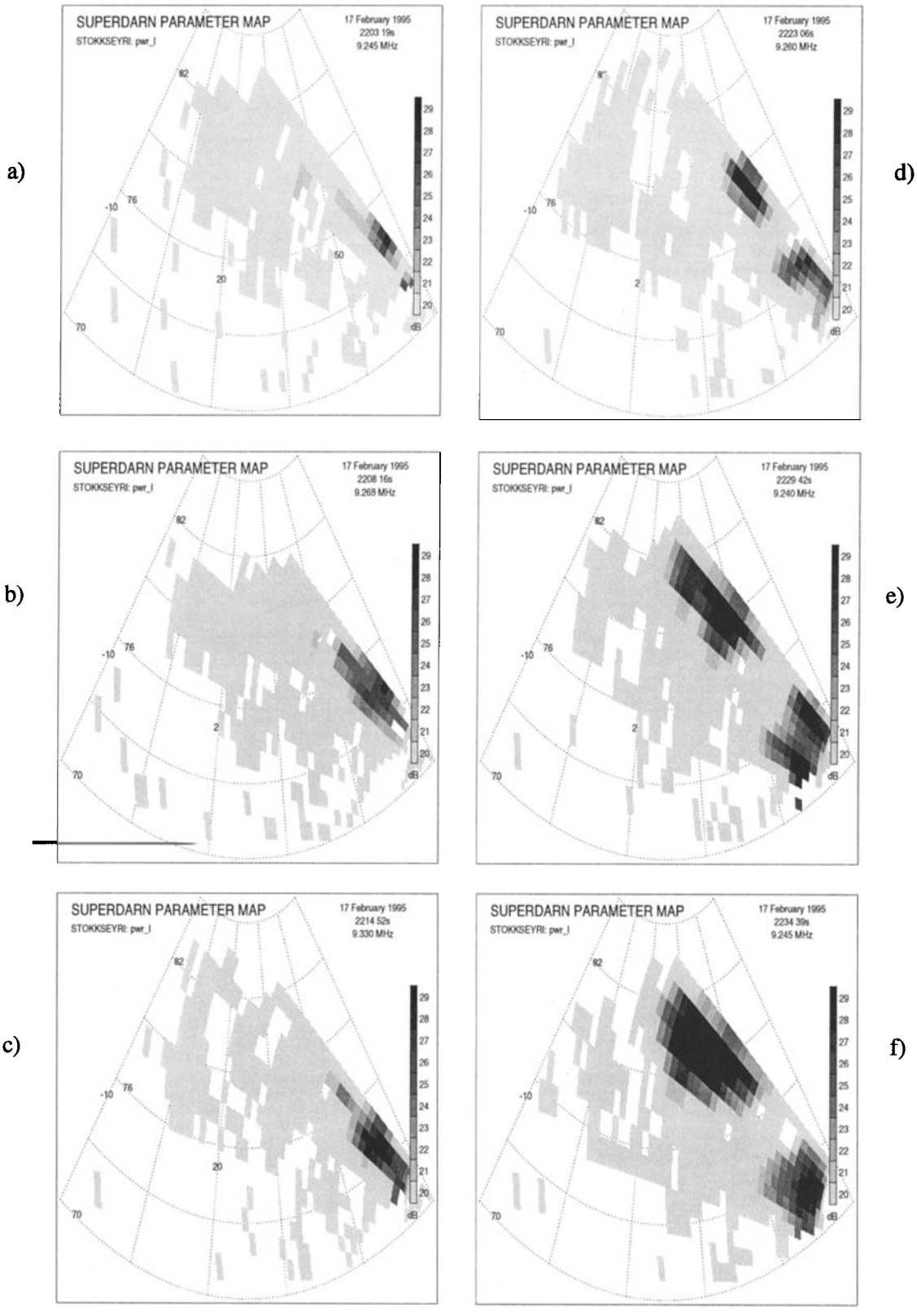

Figure 6. Temporal evolution of the signal-to-noise ratio recorded by the Stokkseyri radar.

($Kp < 1^+$). The structures always appear in a very structured and dynamic convection pattern and are not related to any strong perturbation, such as substorms.

All the structures appear at high latitudes (between 74°and 81°) and in the evening sector (between 1900 and 2100 MLT). Considering the statistical location of the auroral oval during such quiet conditions [*Feldstein and Starkov*, 1967], they are located near the poleward boundary of the

Table 1. Observations Summary

Interplanetary Magnetic Field					Location		Characteristics		
B_x, nT	B_y, nT	B_z, nT	$\|B\|$, nT	*Kp*	MLAT, deg	MLT	Lifetime, min	Size 1, km	Size 2, km
+2.5	-0.5	+2	3.2	1+	75	2100	10	700	no
-6	+2.5	+2	6.8	1+	81	1900	10	300	no
-5	+2	+5	7.3	1-	80	1900	5	200	no
-2	+2	+3	4.1	1-	78	2130	5	250	no
+0.5	-4	+2.5	4.7	1-	74	2130	5	no	no
+1	-2	+1	2.5	1	77	1940	5	300	300

auroral oval, or in the polar cap. Their magnetic latitude is slightly controlled by the magnetic field orientation, going to higher latitudes when B_y is positive and B_x is negative.

The range from the radars is always > 1000 km, suggesting that the observations are taking place in the *F* region (under the hypothesis of a direct propagation). Its characteristic scale size (size 1 and size 2 refer to the size determined by the two radars involved in each event, an undefined size means that it cannot be deduced from the signal-to-noise ratio recorded by the radar) is of the order of 300 km, and it seems to appear during 5 to 10 min without any motion. In all cases, the temporal evolution of the convection pattern suggests that the structure appears at the center of a vortex or a convection reversal, in a region where a divergent electric field is present, induced by a small-scale field-aligned current.

2.3. Artifact Possibility

In all observations the velocity flow is highly divergent, the divergence being $\sim$ 1 order of magnitude larger than the standard values resulting from measurement uncertainties. This contradicts the well-known hypothesis of a divergence-free motion in the *F* region, where the structure is supposed to be observed. *Freeman et al.* [1990] have mentioned several similar observations in the *E* region with the Sweden and Britain Radar Experiment (SABRE) HF radars, when looking to the electron motion. In their cases, observations were unsteady in space and time, and the authors have concluded that structures were not real. Therefore the possibility of an artifact in the radar measurements has to be discussed.

The structures are defined from radial velocities recorded by the radars, which are computed from the autocorrelation function (ACF) of backscattered signals. We examine successively the quality of ACFs and the quality of velocity determination. Another possibility is an error in the assumed location of the structure, due, for example, to a non standard propagation path made of the radar wave.

2.3.1. Autocorrelation function. The ACF quality strongly depends on its number of points and on the zero-lag SNR. When comparing the distribution of the number of points in the ACFs which are recorded inside and outside the structure for all events, it appears that the maximum of the distribution is greater inside the structure (10 points) than outside (7 points). The SNR distributions computed inside and outside the structure show that the data quality is higher inside the structure (15 dB) than outside (8 dB). These results show that the ACF quality should not introduce any bias in the analysis.

2.3.2. Velocity determination. In order to extract the radial velocity information from the ACF one fits the temporal evolution of its phase [*Villain et al.*, 1987]. *Barthes et al.* [1998] have shown that when the velocity spectrum has several components, the error in velocity determination increases. By checking the error distribution inside and outside the structure it is found that these errors are similar and thus that the quality of the velocity determination is sufficiently good to compute the convection map.

2.3.3. Data localization. When computing the standard convection maps [*Cerisier and Senior*, 1994], as well as the high-resolution ones [*André et al.*, 1999], the data localization is of primary importance. The error in localization of radar scatters has already been discussed by *Baker et al.* [1986], *Ruohoniemi et al.* [1987], and *André et al.* [1997]. The first point is to estimate if the error in scatter localization could lead to an erroneous derivation of the velocity field. This is easily estimated by shifting the radial data of one radar in order to destroy the structure in the resulting velocity vector map. This shift is of the order of 140 km, about one half of the structure scale size, and is greater than the expected localization error ($\approx$ 15 km) by 1 order of magnitude. A local perturbation in the ionospheric density can enhance this error to $\sim$ 30 km [*André et al.*, 1997], which is still a much lower value. Only an unusual propagation path, with for example, a 1.5 hop, might give such an error in localization.

2.3.4. Anomalous radar wave propagation. Another error source is a nonstandard propagation, with 1.5 hop mode. The radar data does not exclude such propagation as a large band of ground scatter is present before the structure in all events and at least in one radar. Their location is constant in time. This strongly suggests that the ionosphere is steady during all the periods and that such an anomalous propagation mode will not appear suddenly. The location of the ground scatter band in the data allows us to estimate the ionospheric density profile: With a ray-tracing simulation program and with the appropriate ionospheric density model it is possible to reproduce the ground scatter band on the same location. For example, during the first event the Goose Bay radar data are reproduced by an ionospheric density model defined with a double Chapman layer and plasma

frequencies of 2.5 MHz at 110 km and 6 MHz at 300 km. Such values of plasma frequency are large for nightside conditions but are still reasonable.

With this ionospheric density profile estimation the altitude of the backscatter area associated to high-velocity divergence structure (during this first event) is found. At ~ 2000 km from the radar both E and F region echoes are present, most of them originating from the F region (>60%). This suggests that the observed structure is located in the F region.

The error in data localization, computed from the same model [*André et al.*, 1997], is of the order of 80 km for data located at ~ 2000 km from the radar. This value is still much lower than the critical value computed previously (140 km).

Finally, the possibility of azimuthal deviation due to the presence of an auroral arc has been investigated. Such deviation increases when the angle between the wave vector and the normal to the arc increases. In order to reproduce the ground scatter echoes observed in the radar data and to maximize the azimuthal deviation one has to consider an arc located at ~ 73°MLAT. This suggests that the arc should be aligned with magnetic shells and not Sun aligned. In such geometry the radar beam azimuthal deviation increases when the radar wave vector deviates from the magnetic north direction. In all our events the radar beams associated to the structure observation are directed toward this direction (± 10°). The maximum azimuthal deviation introduced by such auroral arc is evaluated by ray tracing to 50 km, a value lower than the critical one.

It is therefore safe to conclude that determination of the velocity field is not corrupted by erroneous data localization. This analysis strongly suggests that the propagation path is the same before and after the structure formation, and the range is in favor of a F region observation. Moreover, as the radar data show a vortex or a convection reversal before the event, one can conclude that the plasma is moving with an $\mathbf{E} \times \mathbf{B}$ velocity and is mainly magnetized as it should be in the F region. Thus, as the propagation path does not change during the observation, the argument that this structure is observed in the F region is strengthened.

3. Discussion

3.1. Divergence in Velocity Field

The plasma motion in the F region is usually described with two hypotheses. First, the plasma is supposed to be uncompressible. This induces a divergence-free motion in the three-dimensional system. Second, one assumes a collisionless plasma. This hypothesis induces a motion in the $\mathbf{E} \times \mathbf{B}$ direction, in a plane perpendicular to the magnetic field. Then, a divergent velocity field in the F region could be due to a temporal variation of the magnetic field amplitude. An observed velocity field divergence of ~ 7 mHz would lead to a magnetic field decrease of ~ 28,000 nT in 2 min. This unrealistic value suggests that the plasma is no longer moving in the $\mathbf{E} \times \mathbf{B}$ direction.

3.2. Demagnetization

In order to explain the high divergence in velocity, one has to consider a plasma in which the ions are collisionnal and which are therefore moving along the electric field direction. Before the event, one observes a vortex or a convection reversal, meaning that a collisionless plasma motion is controlled by a divergent electric field. Under the same electric field conditions, the motion of a collisional plasma becomes divergent, as observed. Our conclusion is that the events correspond to a change in the ion behavior, from the usual collisionless state to an unusual collisional state. Such a process is called here ion demagnetization. The parameter defining the collisional characteristic of the ions in a plasma is $\kappa = \nu_i/\Omega_i$, where ν_i is the collision frequency and Ω_i is the ion gyrofrequency. The plasma is collisionless when $\kappa < 1$ and collisional in the other case. In the F region, we have usually $\kappa \approx 310^{-3}$. This means that the demagnetization process could occur only after an anomalously strong increase of the collision frequency.

3.3. Electric Field Variations

The value of κ in the demagnetized plasma might be derived from the velocity divergence (7 mHz). If we consider the ion motion in a collisional plasma, one can write the velocity divergence as (1). Here we assume that electron motions along the magnetic field line keep the charge neutrality.

$$\nabla \cdot \mathrm{v} = \frac{\kappa}{1+\kappa^2} \frac{\nabla \cdot \mathbf{E}}{\mathbf{B}} \tag{1}$$

Knowing the velocity divergence, one can derive κ as a function of the electric field divergence. The demagnetization occurs ($\kappa \geq 1$) when the divergence of the electric field has a minimum value of 0.7 μV/m^2. Assuming an homogeneous convection reversal, i.e., a constant velocity amplitude, this minimum value corresponds to an electric field of 20 mV/m, or a plasma velocity of 400 m/s, which is regularly observed in the ionosphere.

3.4. Types of Process

Several factors can create this demagnetization, for example, an increase of the neutral density or modifications of the plasma temperature or composition. The first two processes increase the ion collision frequency, and the last decreases the ion gyrofrequency. Following *Millward et al.* [1993], one can consider a strong heating in the E region, which leads to an increase of the neutral density in the F region (increase of the collision frequency) and change the plasma composition (decrease of the ion gyrofrequency). This process can decrease κ by a factor 6, which is not sufficient to demagnetize the ions in the F region

One can also consider an artificial increase of the ion collision frequency induced by an anomalous transport, characterized by an effective collision frequency ν^*. A new source of free energy gives rise to an instability which leads to the growth of electric field fluctuations in the plasma. When

the electric field amplitude is large enough, some particles are trapped in the wave trains. Then, interactions between the wave trains lead to a brownian motion characterized by an effective collision frequency. This non linear wave particule interaction ends in instability saturation. This anomalous diffusion process is called "neoclassical," as it is well known and confirmed by many experimental studies in tokomaks [e.g., *Horton*, 1984; *Galeev and Sagdeev*, 1984, and references therein].

If the effective collision frequency becomes larger than the ion gyrofrequency, the anomalous transport demagnetizes the trapped ions. The electric field fluctuations modify the trapped particle behavior, but their macroscopic motions are still defined by the macroscopic electric field projected from the magnetosphere. Such a process can demagnetize the *F* region ions and induce a highly divergent flow in a plane perpendicular to the magnetic field.

4. Conclusions

Applying the high-resolution merging technique to SuperDARN data, we have found several unusual mesoscale structures in the ionospheric convection pattern, characterized by a high-velocity divergence in a plane perpendicular to the magnetic field. In all events the structure appears near the poleward boundary of the auroral oval (74°to 81°MLAT and 19°to 21°MLT), when the IMF is northward and during a low magnetic activity.

The temporal evolution of the convection characteristics suggest a very dynamic magnetosphere, with the formation of an electric field shear moving toward the magnetotail and followed by the formation of a divergent electric field. The structure, characterized by this high-velocity divergence, appears at the center of this divergent electric field. Two patches of high SNR are also observed by the radars at the structure boundaries. The temporal evolution of these patches is very well correlated with the formation of the divergent electric field structure. In all events, the structures seem to appear in the center of a divergent electric field. Their scale size, as defined by the SNR, is of the order of 300 km, and their lifetime is between 5 and 10 min.

We have extensively discussed the possibility of an artifact in the radar observations, considering successively the data quality and the data localization for both direct and indirect propagation path. Our conclusion is that those observations do not result from an erroneous velocity vector determination and that the structure is located in the *F* region, where ions are supposed to be magnetized.

The observations are thus in contradiction with the well-known divergent-free plasma motion in the *F* region. In order to explain these structures one has to consider a plasma in which the ions become collisional, as suggested by the divergent electric field structure observed before the events. The structures are then interpreted as the result of localized ion demagnetization in the *F* region. Finally, we have suggested that such a demagnetization can be obtained by an anomalous transport induced by plasma waves interactions. This process will be examined theoretically in more details in a forthcoming paper.

Acknowledgments. The authors wish to thank the data processing team at the Laboratory for Extraterrestrial Physics, NASA Goddard Space Flight Center, for providing IMF data from the IMP 8 and WIND satellites. The Goose Bay and Stokkseyri radars are supported by NSF Grant ATM 9502993 and INSU, respectively. The Saskatoon and Kapuskasing radars are funded by NSERC Canada CSP grant 119615 and NASA grant NAG 5-1099, respectively.

Michel Blanc thanks Kristian Schlegel and A. David M. Walker for their assistance in evaluating this paper.

References

André, R., C. Hanuise, J.-P. Villain, and J.-C. Cerisier, HF radars: Multifrequency study of refraction effects and localization of scattering, *Radio Sci.*, *32*, 153–168, 1997.

André, R., J.-P. Villain, C. Senior, L. Barthes, C. Hanuise, J.-C. Cerisier, and A. Thorolfsson, Toward resolving small-scale structures in ionospheric convection from SuperDARN, *Radio Sci.*, *34*, 1165–1176, 1999.

Baker, K., R. Greenwald, A. Walker, P. Bythrow, L. Zanetti, T. Potemra, D. Hardy, F. Rich, and C. Rino, A case study of plasma processes in the dayside cleft, *J. Geophys. Res.*, *91*, 3130–3144, 1986.

Barthes, L., R. André, J.-C. Cerisier, and J.-P. Villain, Separation of multiple echoes using a high resolution spectral analysis in SuperDARN HF radars, *Radio Sci.*, *33*, 1005–1017, 1998.

Bythrow, P., W. Burke, T. Potemra, L. Zanetti, and A. Lui, Ionospheric evidence for irregular reconnection and turbulent plasma flows in the magnetotail during periods of northward interplanetary magnetic field, *J. Geophys. Res.*, *90*, 5319–5325, 1985.

Cerisier, J.-C., and C. Senior, Merge: A FORTRAN program, *Tech. rep.*, Centre d'Étude des Environnements Terrestres et Planétaires CNRS, 1994.

Crooker, N., Reverse convection, *J. Geophys. Res.*, *97*, 19,363–19,372, 1992.

Crooker, N., and F. Rich, Lobe cell convection as a summer phenomenon, *J. Geophys. Res.*, *98*, 13,403–13,407, 1993.

Cumnock, J., R. Heelis, M. Hairston, and P. Newell, High-latitude ionospheric convection pattern during steady northward interplanetary magnetic field, *J. Geophys. Res.*, *100*, 14,537–14,555, 1995.

Feldstein, Y., and G. Starkov, Dynamics of auroral belt and polar geomagnetic disturbances, *Planet. Space Sci.*, *15*, 209–229, 1967.

Freeman, M., D. Southwood, M. Lester, and J. Waldock, Measurement of field-aligned currents by the SABRE coherent scatter radar, in *Physics of Magnetic Flux Ropes*, *Geophys. Monogr. Ser.*, vol. 58, edited by C. Russel, E. Priest, and L. Lee, pp. 575–580, AGU, Washington, DC.,1990.

Friis-Christensen, E., M. McHenry, C. Clauer, and S. Vennerstrom, Ionospheric traveling convection vortices observed near the polar cleft: A triggered response to sudden changes in the solar wind, *Geophys. Res. Lett.*, *15*, 253–256, 1988.

Galeev, A., and R. Sagdeev, Current instabilities and anomalous resistivity of plasma, in *Handbook of Plasma Physics, Basic Plasma Physics*, vol. 2, edited by M. Rosenbluth and R. Z. Sagdeev, chap. 6.1, pp. 271–303, Elsevier Sci., New York, 1984.

Greenwald, R., W. Bristow, G. Sofko, C. Senior, J.-C. Cerisier, and A. Szabo, Super Dual Auroral Radar Network radar imaging of dayside high latitude convection under northward interplane-

tary magnetic field: Toward resolving the distorted two-cell versus multicell controversy, *J. Geophys. Res.*, *100*, 19,661–19,674, 1995a.

Greenwald, R., et al., DARN/SuperDARN: A global view of the dynamics of high latitude convection, *Space Sci. Rev.*, *71*, 761–796, 1995b.

Heelis, R., P. Reiff, J. Winningham, and W. Hanson, Ionospheric convection signature observed by DE 2 during northward interplanetary magnetic field, *J. Geophys. Res.*, *91*, 5817–5830, 1986.

Horton, W., Drift wave turbulence and anomalous transport, in *Handbook of Plasma Physics, Basic Plasma Physics*, vol. 2, edited by M. Rosenbluth and R. Z. Sagdeev, chap. 6.4, pp. 383–449, Elsevier Sci., 1984.

Kamide, Y., and O. Troshichev, A unified view on convection and field-aligned current patterns in the polar cap, *J. Atmos. Terr. Phys.*, *56*, 245–263, 1994.

Lester, M., O. D. la Beaujardière, J. Foster, M. Freeman, H. Lühr, J. Ruohoniemi, and W. Swider, The response of large scale ionospheric convection pattern to changes in the IMF and substorms: Results from SUNDIAL 1987 campaign, *Ann. Geophys.*, *11*, 556–571, 1993.

Millward, G., S. Quegan, R. Moffet, T. Fuller-Rowell, and D. Rees, A modelling study of the coupled ionospheric and thermospheric response to an enhanced high-latitude electric field event, *Planet. Space Sci.*, *41*, 45–56, 1993.

Reiff, P., and J. Burch, IMF *By* dependent plasma flow and birkeland currents in the dayside magnetosphere, 2, a global model for northward and southward IMF, *J. Geophys. Res.*, *90*, 1595–1609, 1985.

Ruohoniemi, J., and R. Greenwald, Statistical patterns of high-latitude convection obtained from Goose Bay HF radar observations, *J. Geophys. Res.*, *101*, 21,743–21,763, 1996.

Ruohoniemi, J., R. Greenwald, K. Baker, J. Villain, and M. McCready, Drift motions of small scale irregularities in the high-latitude *F* region: An experimental comparison with plasma drift motions, *J. Geophys. Res.*, *92*, 4553–4564, 1987.

Ruohoniemi, J., R. Greenwald, K. Baker, J. Villain, C. Hanuise, and J. Kelly, Mapping high-latitude plasma convection with coherent HF radars, *J. Geophys. Res.*, *94*, 13,463–13,477, 1989.

Ruohoniemi, J., R. Greenwald, O. D. la Beaujardière, and M. Lester, The response of the high-latitude dayside ionosphere to an abrupt northward transition in the IMF, *Ann. Geophys.*, *11*, 544–555, 1993.

Russell, C., and R. Elphic, Initial ISEE magnetometer results: Magnetopause observations, *Space Sci. Rev.*, *22*, 681–715, 1978.

Siscoe, G., What determines the size of the auroral oval?, in *Auroral Physics*, edited by C.-I. Meng, M. Rycroft, and L. Franck, chap. IV-1, Cambridge Univ. Press, New York,1991.

Tagushi, S., and R. Hoffman, Ionospheric plasma convection in the midnight sector for northward IMF, *J. Geomagn. Geoelectr.*, *48*, 925–933, 1996.

Taylor, J., T. Yeoman, M. Lester, M. Buonsanto, J. Scali, J. Ruohoniemi, and J. Kelly, Ionospheric convection during the magnetic storm of 20-21 March 1990, *Ann. Geophys.*, *12*, 1174–1191, 1994.

Tsunoda, R., High-latitude *F* region irregularities: A review and synthesis, *Rev. Geophys.*, *26*, 719–760, 1988.

Villain, J.-P., R. Greenwald, K. Baker, and J. Ruohoniemi, HF radar observations of *E*-region plasma irregularities produced by oblique electron streaming, *J. Geophys. Res.*, *92*, 12,327–12,342, 1987.

R. André, J. P. Villain, and V. Krasnosel'skikh, LPCE/CNRS, 3A Avenue de la Recherche Scientifique, 45071 Orléans Cedex 2, France. (raandre@cnrs-orleans.fr)

C. Hanuise, LSEET/CNRS, Université de Toulon, BP 132, 83957 La Garde, France.

(Received April 28, 1999; revised November 23, 1999; accepted November 23, 1999.)